SSCL-Preprint-89

SSCL-Preprint-89

Superconducting Super Collider Laboratory

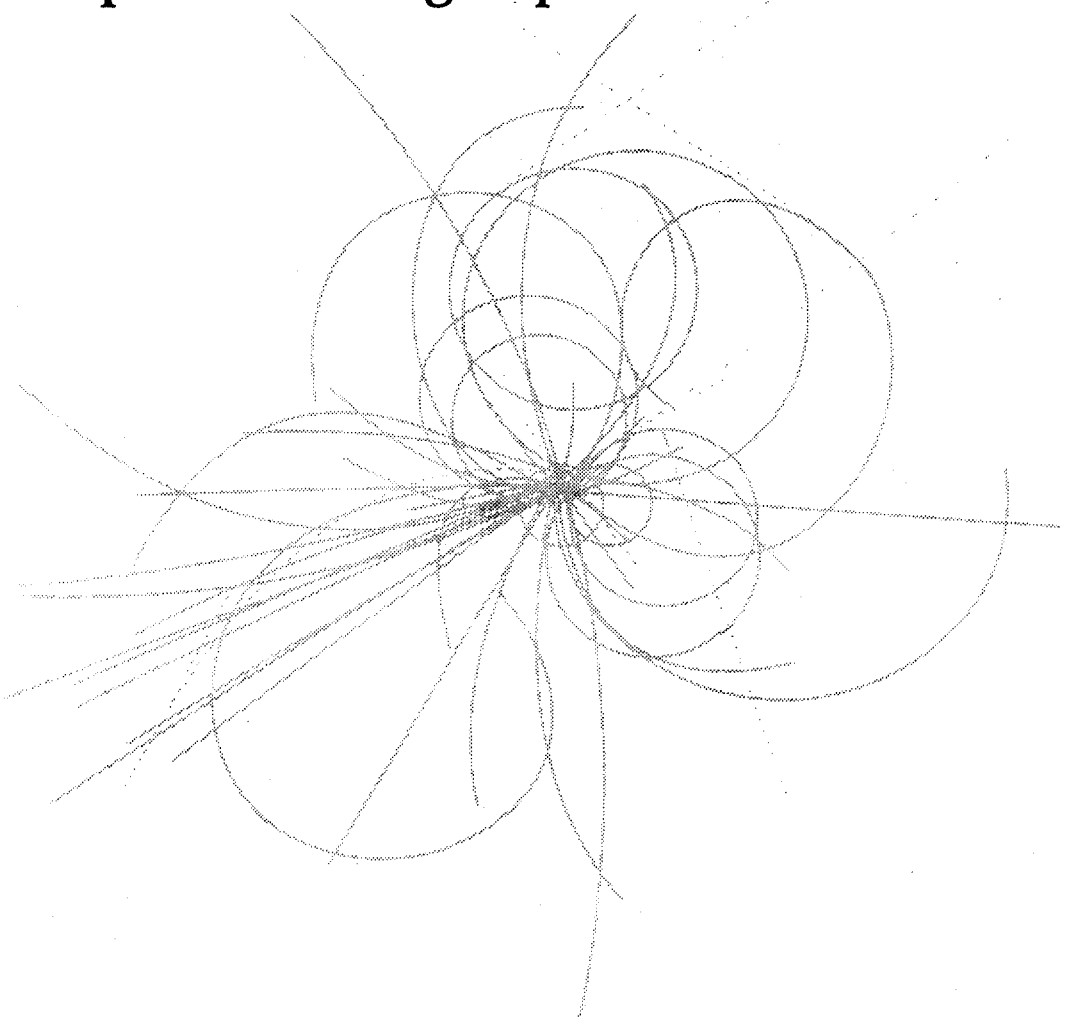

Experimental Issues in Measuring $W_L^+ W_L^+$ Scattering

J. Thomas, E. Wang

August 1992

SSCL-Preprint-89

Experimental Issues in Measuring $W_L^+ W_L^+$ Scattering*

J. Thomas, E. Wang

Superconducting Super Collider Laboratory†
2550 Beckleymeade Ave.
Dallas, TX 75237

August 1992

*Presented at the GEM Collaboration Tucson, AZ, March 1992.

†Operated by the Universities Research Association, Inc., for the U.S. Department of Energy under Contract No. DE-AC02-89ER40486.

Experimental Issues in Measuring $W_L^+W_L^+$ Scattering

J. Thomas, E. M. Wang

August 21, 1992

Abstract

Problems pertaining to the observation of like sign, longitudinally polarized W pairs, due to large backgrounds from $t\bar{t}$ production at SSC are studied within the environment of the two proposed detectors, SDC and GEM. A charge discrimination level of 10^{-5} and a calorimeter isolation rejection factor of 10^{-4} are necessary requirements of any detector which will be used to measure such an excess of W_LW_L pairs.

1 Introduction

Recent phenomenological results concerning the so-called "no lose" scenario [1],[2],[3],[4] indicate that something interesting must be found at the SSC. Either a Higgs resonance below 1 TeV exists, or an excess of longitudinally polarized vector boson pairs at high invariant mass will be seen, indicating that weak interactions have, in some sense, become strong. If neither is seen then a significant descrepency within the Standard Model will have been discovered. The experimental demands of the observation of the most experimentally accessible decay mode, $W_L^+W_L^+$ (where '+' denotes like sign), on SSC detectors are examined in this paper. Further, the observation of W_LW_L scattering will be the first experimental evidence of the existence of Goldstone Bosons [9].[1]

The search for Standard Model Higgs bosons has been discussed numerous times in many SSC workshops [10]. Basically one looks at 2-γ, or 2-Z (4 lepton) decay modes of the Higgs. In the case of high mass WW pairs, the experimental situation has not been as well studied. From parton level calculations, we know that there are significant backgrounds from transverse Standard Model WW pairs and perhaps of even greater significance, the potentially overwhelming production of $t\bar{t}$ events.

2 Physics Review

In principle, one could look at all longitudinal vector boson pairs at high invariant mass in order to establish an excess rate. However, the rates at high mass are very low (a handful at $M_{VV} > 1$ TeV). W bosons offer the most promise due to their higher branching ratio into leptons as compared to

[1] Pions are pseudo-Goldstone bosons due to their non-zero mass.

Z bosons. Lepton decay channels are preferred to assist in good identification of the gauge bosons. Due to the process

$$t\bar{t} \rightarrow W^+W^-b\bar{b} \tag{1}$$

the unlike sign W pair signal is swamped. As studied previously [3] we must resort to the like sign W longitudinally polarized pair as the main viable channel. The signal process (Figure 1) is given by:

$$pp \rightarrow WW \rightarrow W_L^+W_L^+ \tag{2}$$

This is much like two photon scattering in e^+e^- collider experiments. Rates for this have been estimated via various techniques (such as the low energy theorems for pion scattering). The signal is characterized by two high p_T longitudinally polarized W bosons. The W bosons decay into isolated leptons of like charge. The initial quark jets used to produce the incoming WW will have on the order of 100 GeV p_T and in principle, can be used as a "tag". A number of standard model backgrounds exist for this process (Figure 2):

$$qq \rightarrow W^+W^+ \tag{3}$$

$$q\bar{q} \rightarrow W + g \rightarrow W + t\bar{t} \tag{4}$$

Furthermore, a serious detector induced background from $t\bar{t}$ itself may exist:

$$gg \rightarrow t\bar{t} \rightarrow W^+W^-b\bar{b} \tag{5}$$

where one obtains a like charge lepton pair from this event when one of the leptons comes from a W decay and the other comes from a b decay. It will be shown in the following sections that there are potentially two additional types of background from process 5. In one case, one of the b jets is so collimated that it will fake an isolated lepton. In the other case, both Ws decay to leptons (unlike sign), but one has its' sign mismeasured.

Generally, Standard Model W pairs from qq scattering (process 3) will not yield tagging jets, aside from very low p_T radiated gluon jets. Processes 4 and 5 generally have central jets from quarks and no forward jets.

3 Outline

For clarity, we will motivate and outline here the work which has been undertaken in this paper. Dicus et al. [6] have studied one particular background from $t\bar{t}$, that shown in Figure 3 (a) where one W decays to a lepton and one b decays to a lepton of the same sign. In subsequent sections, we will refer to this background as Type 1 background from $t\bar{t}$. Their claim was that a combination of two cuts, that of lepton isolation and forward jet tagging (termed m_{jl} in their publication) would sufficienctly kill this background. However, SDC studies [7] indicate that forward jet tagging destroys 80 % of the signal and so by necessity, we leave out a comprehensive forward jet tagging study in this paper. (It is computationally difficult to check the forward jet tagging with the generator + fragmentation + detector simulation for rejections of order 10^{-4} because a huge amount of CPU time is necessary and we already have a result from SDC which shows its inviability.)

We have identified two further sources of background from $t\bar{t}$:

- Figure 3 (b) shows the second background from $t\bar{t}$ where both Ws decay to leptons (unlike sign), but one has it's sign mismeasured in the tracking detector. Also, the two b jets can look very like the forward "tag" jets. This will be referred to as Type 2 background from $t\bar{t}$.

- Figure 3 (c) shows the third background from $t\bar{t}$ where one W decays to a lepton, as before, and one b jet decays to anything which looks like one track and electromagnetic energy, due to the very collimated b jet. This will be referred to as Type 3 background from $t\bar{t}$.

We have compared the results of reference [6] with our $t\bar{t}$ generator, in order to check the overall normalization. We have determined some cuts (similar to those used in [6], but taking into account certain experimental realities) to make a preselection of high p_T, back to back leptons from $t\bar{t}$ (and $t\bar{t}$ + g) with which to study the effects of the two SSC detectors, GEM [8] and SDC [7], on the background.

The distinction between $t\bar{t}$ and $t\bar{t}$ + g in the text is mostly for definition because the total $t\bar{t}$ cross section consists crudely of a sum of $t\bar{t}$ and $t\bar{t}$ + g. It is unlikely that a $t\bar{t}$ quark pair be formed without being accompanied by a low energy co-linear gluon much like a photon radiates from high energy electrons. However, at generation, it is possible to make a cut on the p_T of the gluon with respect to the quark which we define here as 30 GeV, below which the event is categorized as $t\bar{t}$ and above which it is $t\bar{t}$+g. The value of this cut separates the events into two categories with approximately equal cross sections and is meant to relate physically to events with and without a final state observable jet.

The number of events for one SSC year (10^7 seconds) at a luminosity of $10^{33}\text{cm}^{-2}\ \text{s}^{-1}$ have been considered in all cases. The signal is expected to be very small, in a range between a few, and a few tens of events.

The problems of the following sections pertain to $W \rightarrow e^{\pm}\nu$. In both the proposed SSC detectors, SDC and GEM, the momentum and charge of the muons is known to better precision than the electrons' and the calorimeter does not furnish the main information for the identification process. However, muons alone will not yield a large enough rate to be experimentally measurable (at least over the period of 1-2 years at a luminosity of $10^{33}\ \text{cm}^{-2}\ \text{s}^{-1}$). Therefore, it is necessary to use electrons to increase the signal to 4 times that of muons alone, and it is to this end that we direct our investigation.

4 Cuts

In view of the preceding discussion, the following available observables are chosen to be utilized in reducing the backgrounds:

1. lepton pt and charge

2. lepton rapidity

3. high p_T jet veto

4. lepton isolation

5. charge discrimination

6. forward jet tagging

4.1 Parton Level Cuts

Two scenarios for producing like sign WW pairs have been calculated at the parton level and compared with the background processes and their results are summarized in Table 1.These results can be found in reference [6]. Only the Type 1 background from $t\bar{t}$ has been considered by these authors. The low limit, where a Standard Model Higgs particle of 1 TeV exists produces the smallest number of WW pairs. The second model is that found in PYTHIA [12], due to Dobado, Herrero and Terron [16], which simulates strongly interacting longitudinal Ws. We choose to impose the same cuts as Dicus et al. [6] in order to compare directly with their previous work. A brief description of these cuts will now follow. After a satisfying comparison we change to more experimentally motivated cuts in the next subsections. The number of events for one SSC year at a luminosity of $10^{33}\mathrm{cm}^{-2}\ \mathrm{s}^{-1}$ are shown.

In the first column, events are required to have two leptons of like sign each with $p_T > 75$ GeV and pseudorapidity (η) < 3.5 with invariant mass, $m_{ll} > 300$ GeV. In the second column, the leptons are further required to have an angle between them in the transverse plane whose cosine is $z_{ll} < -0.8$, and whose vector difference in p_T, δp_T^{ll}, > 200 GeV. This will ensure that the events selected contain leptons which are nearly back to back in the transverse plane perpendicular to the beam line. The third column contains events after a high p_T jet veto has been applied. This demands that no event with a jet with $p_T^j > 125$ GeV be accepted. This allows the signal to pass (the spectator jets have typically $p_T^j \leq 100$ GeV), but the background events from $t\bar{t}$ for example, which have other high p_T jets, will not pass.

After the aforementioned cuts, only two other handles were discussed in reference [6] on how to reduce the $t\bar{t}$ and $t\bar{t}$ + g background. The first of these was a cut on the isolation of the lepton and the second was identification of the forward jets. These topics will be addressed in detail in the following subsections.

Our $t\bar{t}$ generator is called PAPAGENO [11] and is shown in Table 1 (numbers in parenthesis) to reproduce the results of Dicus et al. with very good agreement.

4.2 Experimentally Motivated Cuts

The above cuts have been used as a basis but the geometries of the two proposed detectors have been used to determine the optimal cuts, most notably the tracking volume of the proposed detectors is smaller than assumed in [6].

4.2.1 Lepton Rapidity and charge

The lepton rapidity distributions for $W_L W_L$, and $t\bar{t} \rightarrow WWb\bar{b}$ of Type 1 and Type 2, restricted to $p_T > 75$ GeV, are shown in Figure 4 for top masses of 150 GeV and 200 GeV. Each event has one entry, that of the higher rapidity lepton. In order to measure the charge of the leptons, it is necessary to cut at a rapidity $\eta < 2.5$ in order to properly utilize the sign measuring capability of

an inner tracker. A value of 2.5 is taken as a ballpark figure similar to that of the SDC and GEM detectors.

4.2.2 Lepton p_T

The lepton p_T distributions, restricted to $\eta < 2.5$, for $W_L W_L$, and $t\bar{t} \rightarrow WWb\bar{b}$ of type 1 and type 2 are shown in Figure 5 for top masses of 150 GeV and 200 GeV. Each event has one entry, that of the highest p_T lepton. It can be seen that a p_T cut of 75 GeV (as recommended in [6]) reduces the signal by $\approx 40\%$ of its original significance, but reduces the background by $\approx 80\%$. In addition, the invariant mass of the lepton pair m_{ll} is required to be > 300 GeV as shown in Figure 6 (including the p_T and η cuts). In addition, the cosine of the angle between the two leptons in the transverse plane, z_{ll} is required to be < -0.8. and the vector difference in p_T, δp_T, between the two leptons must be > 200 GeV. These variables are shown in Figures 7 and 8 for type 1 and type 2 background from $t\bar{t}$ and $t\bar{t} + g$ respectively. A top mass of 200 GeV is used, and the effects of the cuts are documented in Table 2.

4.2.3 High p_T Jet Veto

After imposing kinematic cuts on the leptons, the jet activity in the event may be studied. The $W_L W_L$ signal should have only two jets in the forward direction and no jets with a large p_T. A jet is defined by coalescing partons within a cone of $R = \sqrt{\Delta\eta^2 + \Delta\phi^2} < 0.5$ and using the resultant 4-momentum sum. A cut is imposed on the events such that the largest p_T jet in the event must have $p_T < 125$ GeV. The distributions for the background and signal (for an arbitrary number of events just for comparison) are shown in Figure 9. Table 2 documents the effects of this cut.

At this point we are left with a few signal events and about one thousand $t\bar{t}$ and $t\bar{t} + g$ events which have like sign. These cuts are what we use to provide our preselected events which we use later to estimate the effects of further cuts.

4.2.4 Lepton Isolation

We now turn specifically to the subject of lepton isolation. In the case of type 1 background from $t\bar{t}$, the lepton from the W is isolated, but the lepton from the b meson is not. Figure 10 shows the energy of b quarks in $t\bar{t}$ + g events after a cut on the b quarks' $p_T > 75$ GeV. Some number of the b quarks are strongly boosted and may give rise to very collimated jets. In the case of the calorimeter, the normal isolation cuts used for jet rejection typically involve summing the energy E_T in a cone around a given candidate calorimeter cell. This is going to be impossible if all the energy is in one cell because the particles from the b jet are too near to the lepton.

The calorimetric isolation studies were performed as follows. First, $t\bar{t}$ events were generated and the b quarks were forced to decay to an electron + X. These events were put through the preselection cuts described earlier. Using the 4 vectors of the particles we look at the mean separation of the lepton and the rest of the b jet by plotting the transverse energy (E_T) inside two annuli sizes (0.01< R <0.25 and 0.05 <R< 0.25) as in Figure 11. We find a drastic change in rejection resulting from the fact that the particles of the b jet lie within R < 0.05 of the lepton because the b jet is so highly collimated.

We subsequently propagate the particles through a fast shower parametrization imbedded into GEANT with geometry similar to SDC. We deposit energy into the electromagnetic and hadron towers segmented by $\eta\phi$ = 0.5 x 0.5 with a parametrization of longitudinal shower shape based on CDF test beam data and which includes fluctuations. The transverse shape was calculated by Fluka [10]. Pileup is included and the effects of previous pulses are weighted by either a fast bi-polar shaping function (= +1 for 1st bucket, -$\frac{1}{2}$ for the next two buckets) with approximately 15 ns peaking time, [17]) or a slow bi-polar shaping (a shape adapted from a liquid argon study of Cleland et al [18]) with 100 ns peaking time. We form a 2 x 2 EM "core" cell around the lepton from the B meson and then calculate ΣE_T(hadronic and electromagnetic) in a four cell wide border surrounding this 2 x 2 core. This is plotted in Figure 12 for these background events and in Figure 13 for the $W_L W_L$ signal for comparison.

We find that a collimated b jet is more easily rejected because the energy is smeared over a wider region and so evidence for a b jet in neigbouring cells can be observed. It is clear from Figure 13 that the cut in ΣE_T must be made at about 3-4 GeV. From Figure 12, it can be seen that this results in a rejection in the range 10^{-2} - 10^{-3}. This result is somewhat shy of the rejection needed to reduce our 1000 preselected events to a negligible level.

The main problem then, is that of recognizing if there *is* a jet at all in the calorimeters rather than determining whether the lepton is isolated. Looking at the fraction of energy in the hadron calorimeter would give an indication that there were hadrons present, and therefore a jet, but this will only be present some of the time. Figure 15 shows the angle, Θ_{max} between the most separated charged tracks in b jets with p_T > 100 MeV (to discard loopers) versus the fraction of hadronic energy in the jet. The jets were fragmented using ISAJET and no attempt has been made to simulate the deposition of energy in the calorimeter so this is really a very optimistic view. The lower plot shows a subset of events with $\Theta_{max} < 0.02$ and the fraction of hadronic energy < 0.25 which represents 1.0% of the total b jets.

In regions covered by the tracking detector, tracking information can be used to help identify that there is indeed a jet, although measuring tracks inside jets with this degree of collimation could essentially be impossible. A very naive estimation can be done by looking at the segmentation of the tracking detectors at the outer radius. We note that this leaves out some handles which may help in identifying jets. Both detectors have silicon trackers at their inner radii which have extremely good position resolution, and may be able to resolve the tracks from the jets. Further, in the case of GEM, the dE/dX information which in principle is available, has not been used. In this sense, this estimate is rather pessimistic. On the other hand, we have assumed that only tracks falling inside one pad in the case of GEM cannot be resolved, but in reality this is much worse, a single track deposits charge on three pads, not just one. In this sense, our estimate is optimistic. SDC, using straw chambers of 4mm diameter, subtents an angle of 2 mrad at an outer radius of 1.6 m. GEM, using Interpolating Pad Chambers, subtends an angle of 7 mrad, using pad widths of 5 mm. We estimate then that in the case of SDC, there are 0.3% and in the case of GEM, 0.5%, of b jets sufficienctly collimated to elude the tracker altogether.

Looking at the Type 1 events which pass the cuts in Table 1 we can estimate the magnitude of this background, because we assume that the topology will be very similar, except that the b quark will not decay semi-leptonically, but hadronically which will multiply the rate by factor 10.

About 1000 Type 1 events pass the cuts which translates into 10000 for this Type 3 background. 0.5% of this constitutes a background on the order of 50 events.

However, a study of this subject in any greater depth, (for example, a detailed simulation of hit generation in the trackers including pileup events or a simulation of the influence on this background of a shower max detector as proposed by SDC) is beyond the scope of this paper, although we hope to have stressed that a problem exists for a detector which has not been designed with the possibility that b jets can look like isolated leptons in mind.

4.2.5 Charge Discrimination

A facet not considered in the various parton level calculations is now discussed. We know that from 150 million $t\bar{t}$ events per year, about 1.5 million will yield WW into an unlike sign, single lepton mode such as e^+e^-. One feature of particle detectors is that there is an inherent limit to how well the charge is measured which comes directly from the size of the magnetic field and the position resolution of the detector. If one of the leptons in process 1 has its' charge mismeasured, the event will look much like the signal. A comparison is made of the proposed tracking detectors for SDC and GEM. At this time, it is unfortunately not possible to put the generated events through the rigors of pattern recognition, and so a "best of all possible worlds" scenario is embraced where we assume perfect hit and pattern recognition, and we study only the shortcomings of the inherent sign selection capabilities of each detector. $t\bar{t}$ and $t\bar{t}+g$ events are generated corresponding to a luminosity of 1 years' running at $10^{33} cm^2 - s^{-1}$ with a top mass of 200 GeV and the preselection cuts are imposed on the events, except that of lepton charge. The high p_T leptons are propagated through the tracking detectors and hits are generated according to the position resolution of each layer as given in references [7] and [8]. A circle fitter adapted from TASSO is used to fit the track to the smeared hits in order to get a measure of the p_T. The higher the p_T of the track, the harder it is to measure the sign of the curvature. To this end, a maximum p_T cut, p_T^{max} is applied to the highest p_T lepton. Tables 3 and 4 show the percentage of signal events as a function of rapidity cut and p_T^{max} cut for two models of strongly interacting Ws. Table 3 shows predictions from the model of Dobado, Herrero and Terron [16] which is found inside PYTHIA and Table 4 shows the predictions of Chanowitz' "linear model" [15].

It can be seen from Tables 3 and 4 that a cut on p_T^{max} of 700 GeV can be imposed without much loss of signal. Also, discrepencies between the two models (probably due to different distribution functions in the generation) are less apparent inside the region of $\eta < 2.5$, $p_T^{max} < 700$ GeV (there is a 10 % difference). Figure 16 shows the curvature (1/r) for GEM and SDC after the geometrical cuts of the detector and the maximum p_T cut have been applied. In the case of SDC, no tracks are seen with the wrong sign. However, about 300 have the wrong charge assignment in the GEM case. It should be emphasized that this simulation does not take into account the non-gaussian tails in the curvature distributions produced after pattern recognition by the wrong assignment of hits to tracks and the effects of delta rays, and that the real life situation can only be worse than this for both SDC and GEM.

4.2.6 Forward Jet Tagging

The last cut expected to be useful in reducing the background in reference [6] is forward jet tagging. The notable features are that the spectator jets are predominantly in the forward direction for the signal but in top events they are mostly in the central region. However, the 10^{-4}-10^{-5} rejection obtained by the ideal parton level calculations in reference [6] has been shown by SDC [7]to be too optimistic as partons fragment into jets producing fluctuations which reduce the effectiveness of the cuts, as well as problems associated with making good jet measurements at high rapidity. Their results showed that the use of a forward jet tag to identify the signal events results in an 80% reduction in efficiency which leads to an unacceptable reduction in signal rate. However, were we nevertheless to attempt some kind of forward jet tag, some Type 2 $t\bar{t}$ events would indeed have one or two b jets which pass the central jet veto cut, where the jet(s) was in the forward region (5 $> \eta >$ 2.5). It can be seen in Figure 10 that the spectrum of b jet energy extends above 1 TeV and so these jets can look exactly like the forward jets of the signal when one of the leptons has its sign mismeasured. Imposing the criteria that both b quark jets lie in the region $2.5 < \eta < 5.0$, in the case of the GEM detector, the number of events having a mismeasured lepton is reduced to the order of a few tens of events, still unacceptable compared to the expected size of the signal. For this reason, jet tagging has not been studied in any further detail especially as it is computationally difficult to check forward jet tagging with the generator + fragmentation + detector simulation for rejections of order 10^{-4} because a huge amount of CPU time is necessary and we already have a result from SDC which shows its inviability.

4.3 Summary

We have started with the parton level cuts of reference [6] and have explored their effects in the experimental environment. Some of the discussion (subsections 4.2.1 - 4.2.3) were common to both GEM and SDC detectors. However, the cuts on lepton isolation and charge selection are very dependent on the detector design. We have attempted to *estimate* the effects of isolation cuts in both the calorimeter and the tracking devices of both detectors in Table 5 along with the effects of the charge selection determined in subsection 4.2.5. We have made the following assertions in the estimation:

- a rejection of between 10^{-2} to 10^{-3} is assumed in the calorimeter for rejecting Type 2 background.
- a rate of 10 times that of Type 2 is expected for the Type 3 background. This represents then events where one b quark decays to jets (with no lepton) and one W decays to a lepton. The jets are very collimated and in addition have a hadronic energy profile such that the only part of the detector which could detect the presence of a jet is the tracker. It is asummed that 0.3% (SDC) and 0.5% (GEM), of the b jets elude the tracking detectors alltogether.

5 High Luminosity Running

As an additional consideration, we note that the low event rates for high mass WW searches might call for higher luminosity running. Is this sensible? We use the same simulation of the calorimeter as previously described and add the appropriate increase in pileup using now the fast shaping time of 15 ns. The concern here is that within a given isolation cone, where we are expecting inactivity, we now have 10 times the energy from low p_T pileup. We must change the cut so that we keep the signal and reject the background. The isolation energy distributions appear in Figure 14. We now adjust the cut so we retain the signal and find that the $t\bar{t}$ rejection is reduced by a factor of 10! Additionally, we impose cell cuts of 1 GeV and replot the isolation. This only helps by a small factor. This would infer that the WW scattering experiment is probably *not* a high luminosity experiment, although a study to find the optimal luminosity with which to see the signal might be useful. Also, to search for the $Z_L Z_L$ signal might be more worthwhile at higher luminosities.

6 Conclusions

The $W_L^+ W_L^+$ search is fundamental to understanding Electroweak Symmetry Breaking and must be performed *in addition* to the search for a light Higgs resonance. The special demands that this physics places on detectors is not trivial. The main procedures which enable us to identify the like sign, $W_L W_L$ signal and reject the background are lepton isolation and jet identification. We find that we need an isolation rejection factor of order 10^{-4} to rid ourselves of the type 1 $t\bar{t}$ and $t\bar{t} + g$ background. The whole procedure falls into serious doubt because the b jets are so collimated. Including tracking information can help at some level if the two track resolution of the tracker is better than the spacial extent of the b jet. A charge discrimination level of 10^{-5} for the spectrum above 75 GeV is needed to reject the type 2 $t\bar{t}$ and $t\bar{t} + g$ background. In conclusion, SDC seems almost equipped to measure the like sign $W_L W_L$ signal, but the present design of GEM is swamped by background.

Initial work for the present study was begun at the U.C Davis Workshop on Higgs/EWSB Physics at Hadron Supercolliders in July 1991.

7 Acknowledgements

We are indebted to Lynne Orr for calculating the $t\bar{t} + g$ cross sections and furnishing us with a working Monte Carlo for this process. We would like to thank Mike Chanowitz for useful comments and for the contents of table 4. We would like to thank Frank Paige and Bryan Lynn for useful discussions as usual.

References

[1] Lee et al., Phys. Rev. D16, 1519 (1977)

[2] Chanowitz and Gaillard, Nucl. Phys. B261, 379 (1985)

[3] Chanowitz and Golden, Phys. Rev. Lett. 61, 1053 (1977)

[4] Barger et al., Phys. Rev. D42, 3053 (1990)

[5] M.S.Berger and M.S.Chanowitz, Phys.Lett. B 263 (1991) 509

[6] D.A.Dicus et al. SLAC-PUB-5599 (1991)

[7] SDC Technical Design Report

[8] GEM baseline 1, GEM TN-92-76

[9]
- J.Goldstone,Nuovo Cimento 19,1961 p15
- Y.Nambu and G.Jona-Lasinio, Phys Rev 122, 1961 p345
- Y.Nambu and G.Jona-Lasinio, Phys Rev 124, 1961 p246
- J.Goldstone, A.Salam and S. Weinberg, Phys ReV 127, 1962 p965

[10] Snowmass 86,88

[11] PAPAGENO version 3.52. I.Hinchcliffe, LBL Internal Communication

[12] PYTHIA version 5.5

[13] J.Thomas and E.M.Wang GEM-TN-92-65. 1992

[14] L.Orr, private communication

[15] M.Chanowitz, private communication

[16] A.Dobado, M.J.Herrero, J.Terron, CERN-TH 5670/90, FTUAM/08-90, CERN-TH 5813/90

[17] Private Communication.

[18] W.E.Cleland et al., Symposium on Detector Research and Development for the SSC, Fort Worth, 1990

like sign lepton source	*# events for 1 year running at $L=10^{33}cm^{-2}\ s^{-1}$*		
	p_T >75GeV,η < 3.5,M_{ll} > 300GeV	$z_{ll} \leq -0.8$, $\delta p_T^{ll} \geq 200$	p_T^j < 125GeV
$W_L W_L$ (1 TeV ϕ^0)	2.8	2.5	1.9
$W_L W_L$	10.2	9.3	7.0
g-exchange	3.5	1.6	0.2
*Type*1 $t\bar{t}$	2541(2549)	2178(2218)	823(734)
*Type*1 $t\bar{t}$ + g	2420	2009	480

Table 1: Like sign lepton sources (electrons only) after parton level cuts from Dicus et al. including a comparison with $t\bar{t}$ events generated with PAPAGENO in parenthesis. Two estimates for $W_L W_L$ production are shown, the lower number being produced when a Standard Model Higgs at 1 TeV exists and the larger number produced in the strongly interacting model generated by PYTHIA.

like sign lepton source	*# events for 1 year at $L=10^{33}cm^{-2}\ s^{-1}$*		
	p_T >75GeV,η < 2.5,M_{ll} > 300GeV	$z_{ll} \leq -0.8$, $\delta p_T^{ll} \geq 200$	p_T^j < 125GeV
Type 1 $t\bar{t}$(Wb)	2178	1936	637
Type 2 $t\bar{t}$(WW)	11253	9559	4429
Type 1 $t\bar{t} + g$(Wb)	2178	1857	476
Type 2 $t\bar{t} + g$(WW)	11374	8712	3025

Table 2: $t\bar{t}$ and $t\bar{t}$+g background sources (electrons only) after experimentally motivated cuts. $t\bar{t}$ events generated with PAPAGENO and $t\bar{t} + g$ events generated with TDECAY.

P_T^{max} *cut/* η *cut* *GeV*	1.0	1.2	1.4	1.6	1.8	2.0	2.2	2.4	2.6	2.8
200.	0.03	0.03	0.05	0.05	0.05	0.05	0.05	0.05	0.05	0.05
300.	0.17	0.20	0.22	0.24	0.24	0.24	0.24	0.24	0.24	0.24
400.	0.25	0.31	0.34	0.38	0.39	0.39	0.39	0.39	0.39	0.39
500.	0.33	0.39	0.44	0.47	0.50	0.50	0.51	0.51	0.51	0.51
600.	0.39	0.46	0.51	0.56	0.59	0.60	0.63	0.63	0.63	0.63
700.	0.40	0.50	0.55	0.60	0.64	0.66	0.72	0.72	0.72	0.72
800.	0.42	0.52	0.57	0.63	0.68	0.71	0.76	0.76	0.76	0.76
900.	0.43	0.54	0.60	0.66	0.71	0.74	0.80	0.80	0.81	0.81
1000.	0.44	0.55	0.61	0.67	0.73	0.76	0.82	0.83	0.84	0.84

Table 3: Percentage of signal as a function of p_T^{max} and η cut for the model of $W_L W_L$ scattering in PYTHIA.

P_T^{max} cut/ η cut GeV	1.0	1.2	1.4	1.6	1.8	2.0	2.2	2.4	2.6	2.8
200.		0.06	0.08	0.10	0.12	0.14	0.16	0.18	0.19	0.21
300.		0.12	0.16	0.20	0.25	0.29	0.33	0.36	0.39	0.41
400.		0.17	0.23	0.30	0.36	0.41	0.46	0.51	0.55	0.58
500.		0.22	0.29	0.37	0.44	0.51	0.57	0.62	0.66	0.70
600.		0.26	0.34	0.43	0.51	0.59	0.65	0.71	0.75	0.79
700.		0.30	0.40	0.50	0.60	0.68	0.76	0.81	0.86	0.90
800.		0.32	0.42	0.53	0.62	0.71	0.78	0.84	0.89	0.93
900.		0.33	0.44	0.54	0.64	0.73	0.80	0.86	0.91	0.95
1000.										

Table 4: Percentage of signal as a function of p_T^{max} and η cut for Chanowitz' linear model

	# events for 1 year running at $L=10^{33}cm^{-2}\ s^{-1}$					
cut	SDC			GEM		
	TYPE 1	TYPE 2	TYPE 3	TYPE 1	TYPE 2	TYPE 3
From Table 2	637 + 476	4429 + 3025	6000 + 4760	637 + 476	4429 + 3027	6000 + 4760
Sign selection	1113	0	10000	1113	300	10000
Isolation in Cal	1 - 10	0		1 - 10	300	
Isolation in tracker	1 - 10	0	30	1 - 10	300	50
Total **estimated**	30 - 40			350 - 360		

Table 5: An estimation of the effects of the cuts for the different experimental configurations of GEM and SDC. The assumptions made in order to reproduce this table are listed in section 4.3

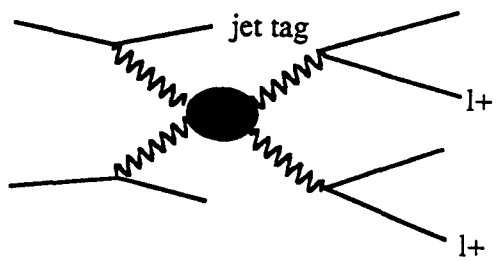

Figure 1: $pp \to WW \to W_L^+ W_L^+$

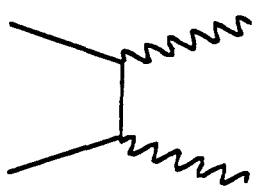

$qq \to W^+ W^+$

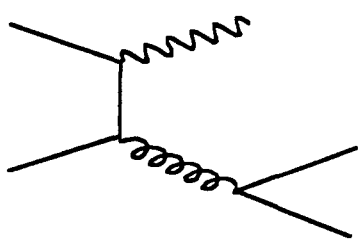

$q\bar{q} \to W^+ + g$

$\to t\,\bar{t}$

Figure 2: $qq \to W^+W^-$ and $q\bar{q} \to W + g \to W + t\bar{t}$

a.

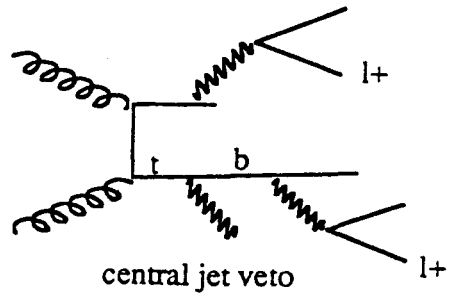

b.

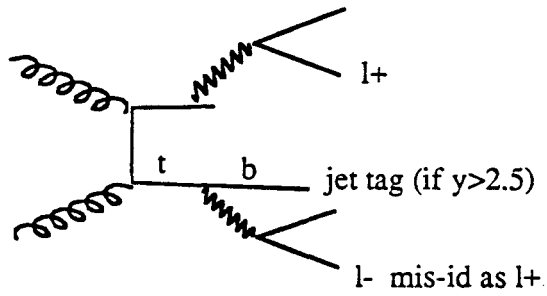

c.

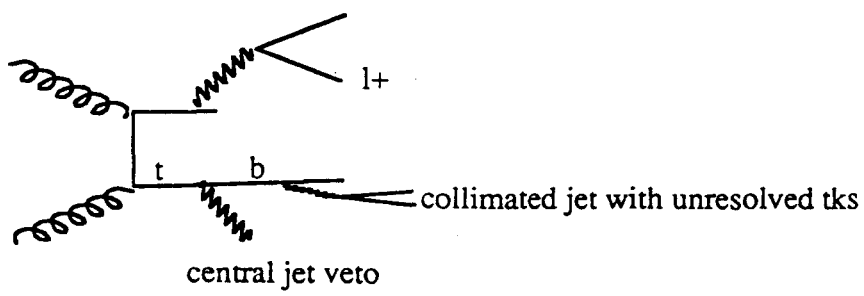

Figure 3: Background processes from $t\bar{t}$ events.

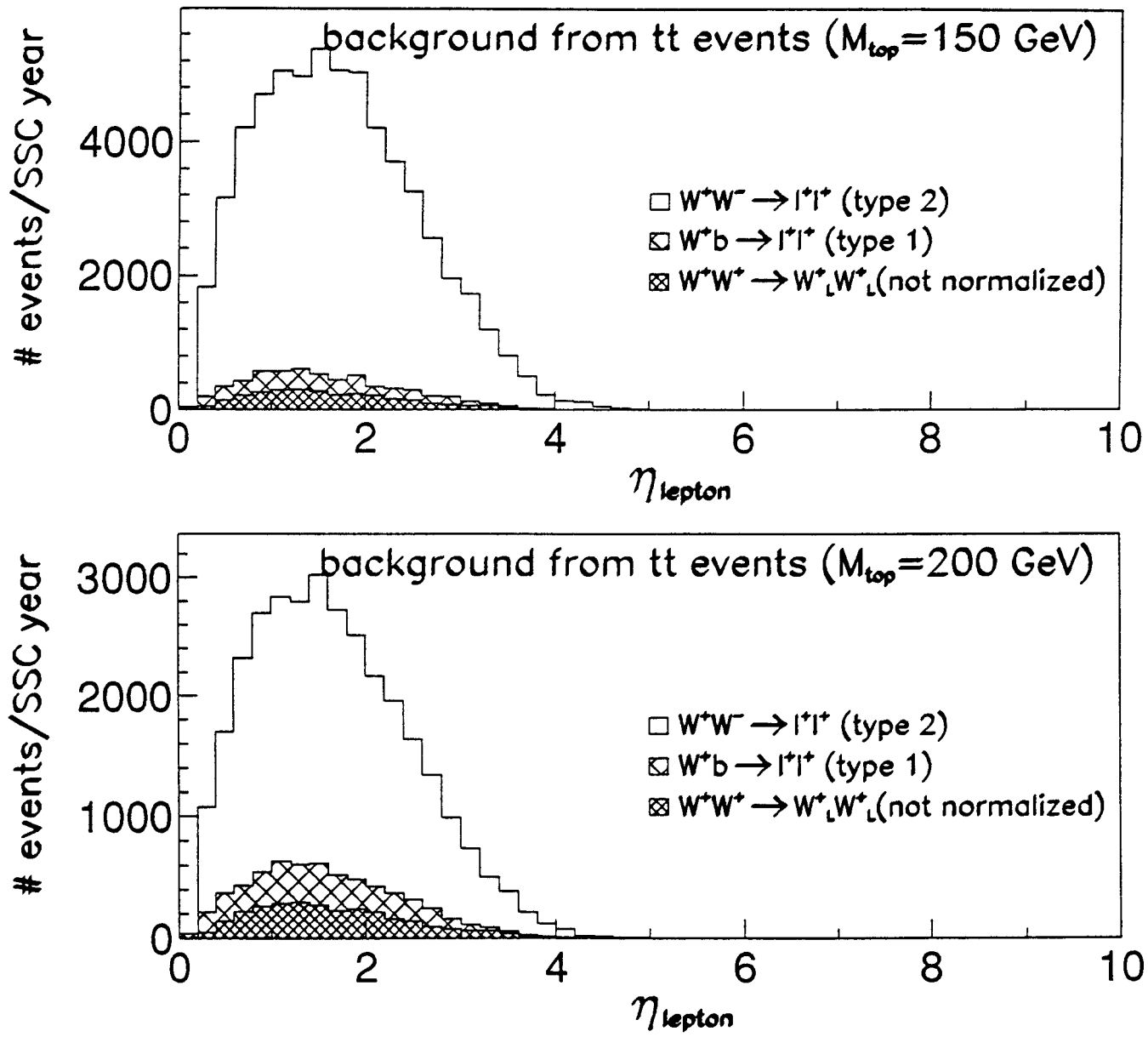

Figure 4: rapidity distributions of most forward lepton from $t\bar{t} \rightarrow WWb\bar{b}$ after $p_T > 75$ GeV cut for m_{top} = 200 GeV and m_{top} = 150 GeV. The unnormalized signal is shown for comparison.

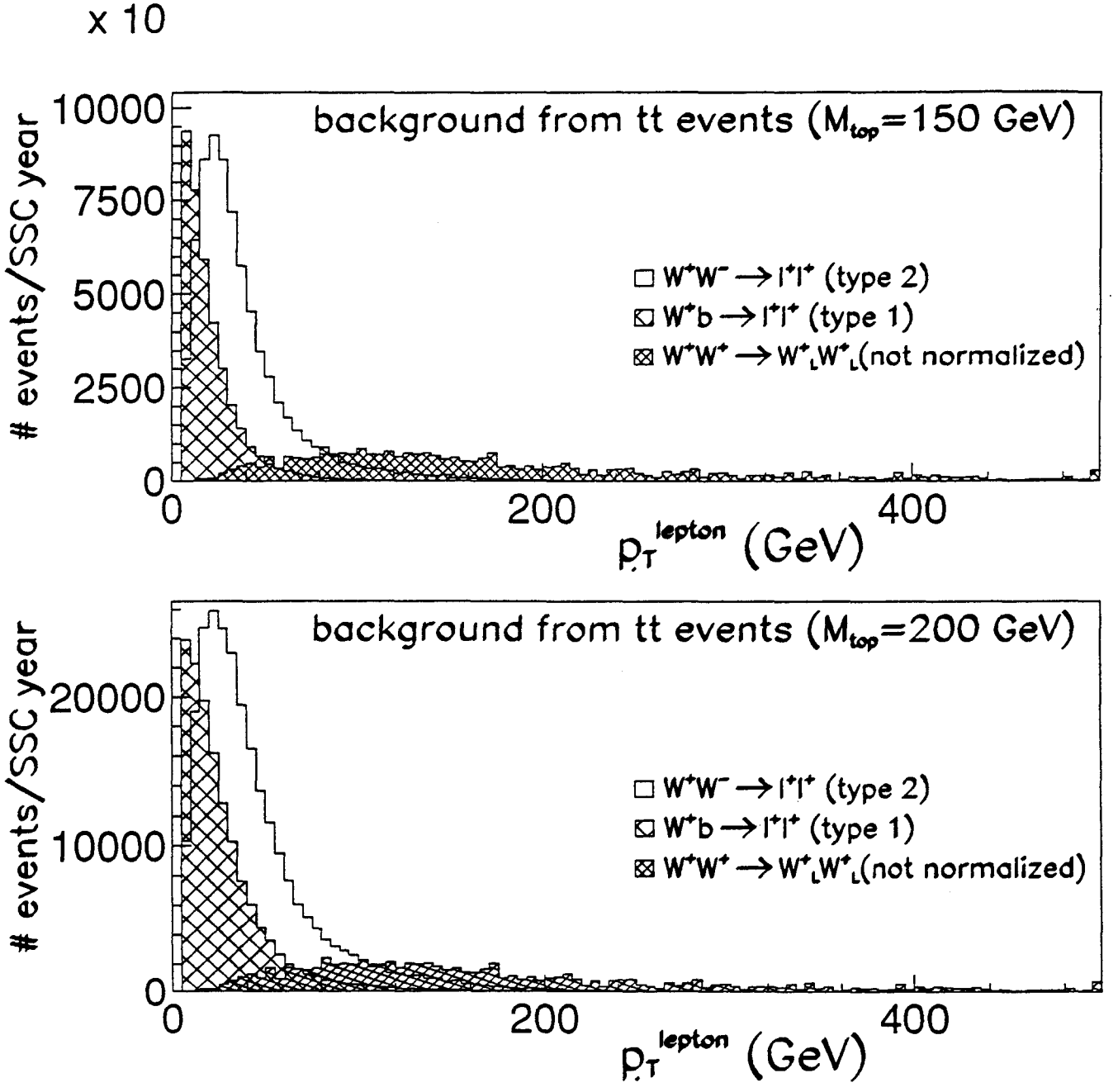

Figure 5: p_T distributions of the highest p_T lepton from $t\bar{t} \rightarrow WWb\bar{b}$ after $\eta < 2.5$ cut for m_{top} = 200 GeV and m_{top} = 150 GeV. The unnormalized signal is shown for comparison.

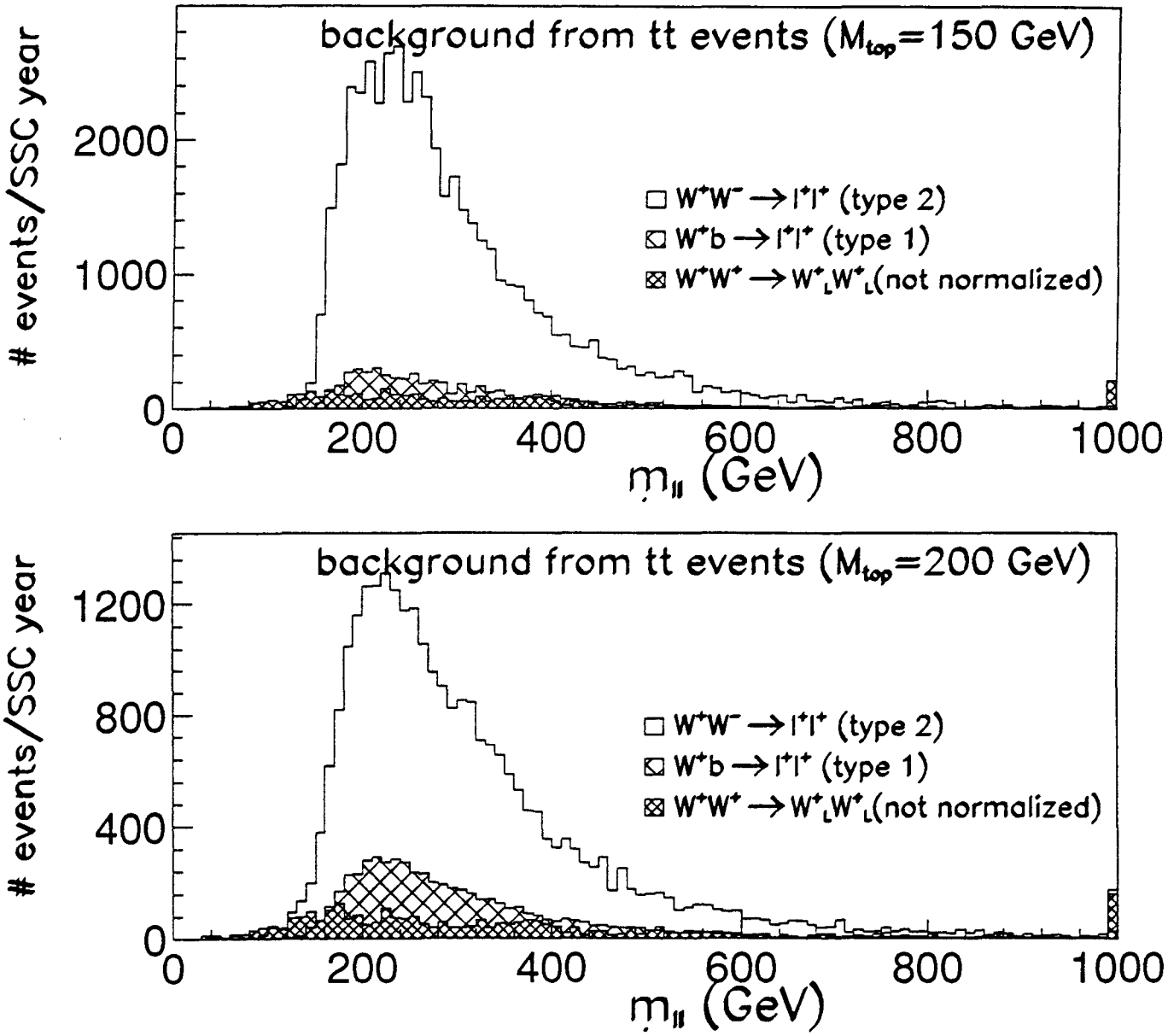

Figure 6: Invariant mass of the two leptons in $t\bar{t}$ background events, m_{top} = 200 GeV and M_{top} = 150 GeV after p_T and η cuts. The unnormalized signal is shown for comparison.

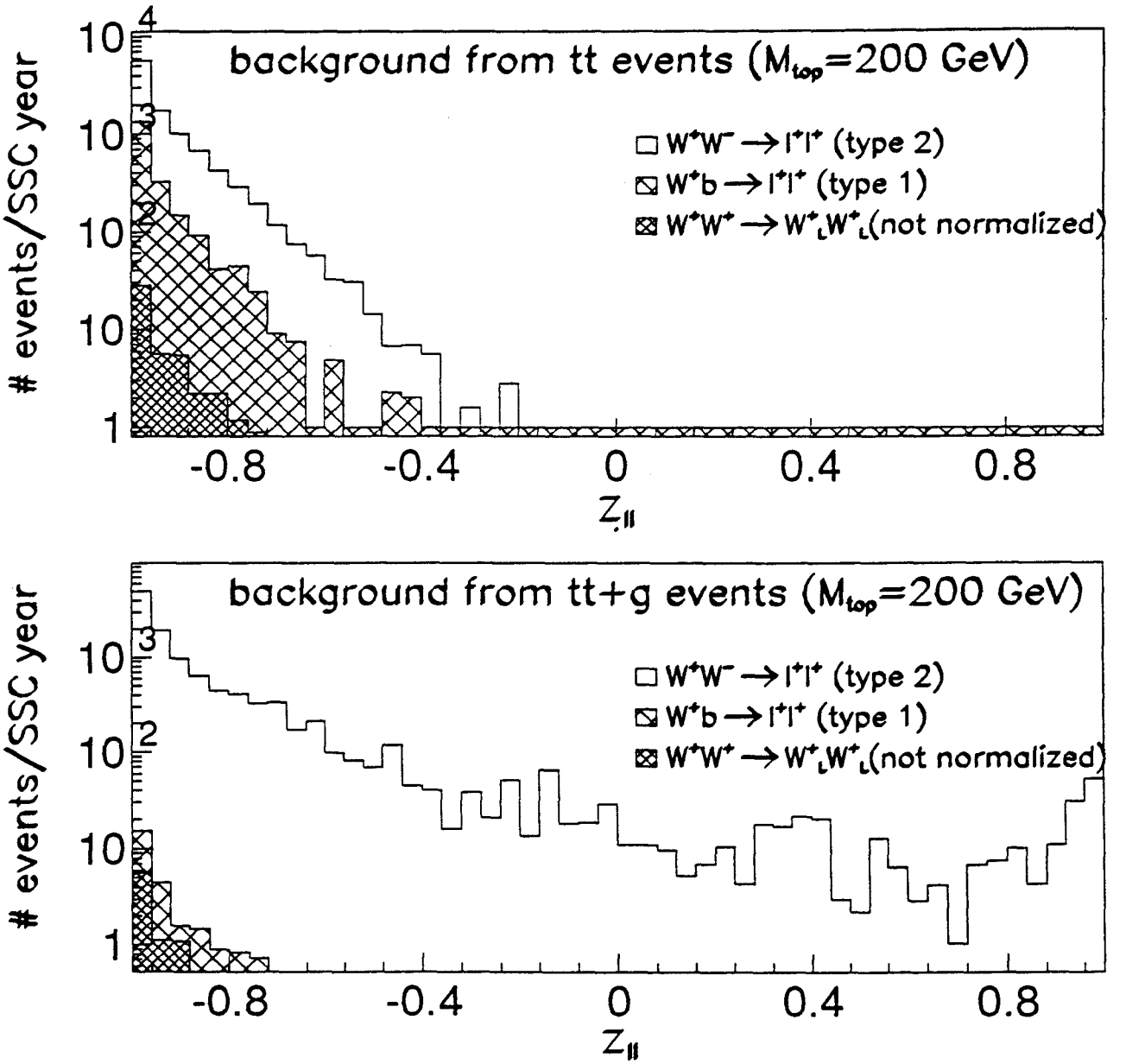

Figure 7: Cosine of the transverse angle between the leptons in $t\bar{t}$ and $t\bar{t} + g$ background events, m_{top} = 200 GeV. The unnormalized signal is shown for comparison.

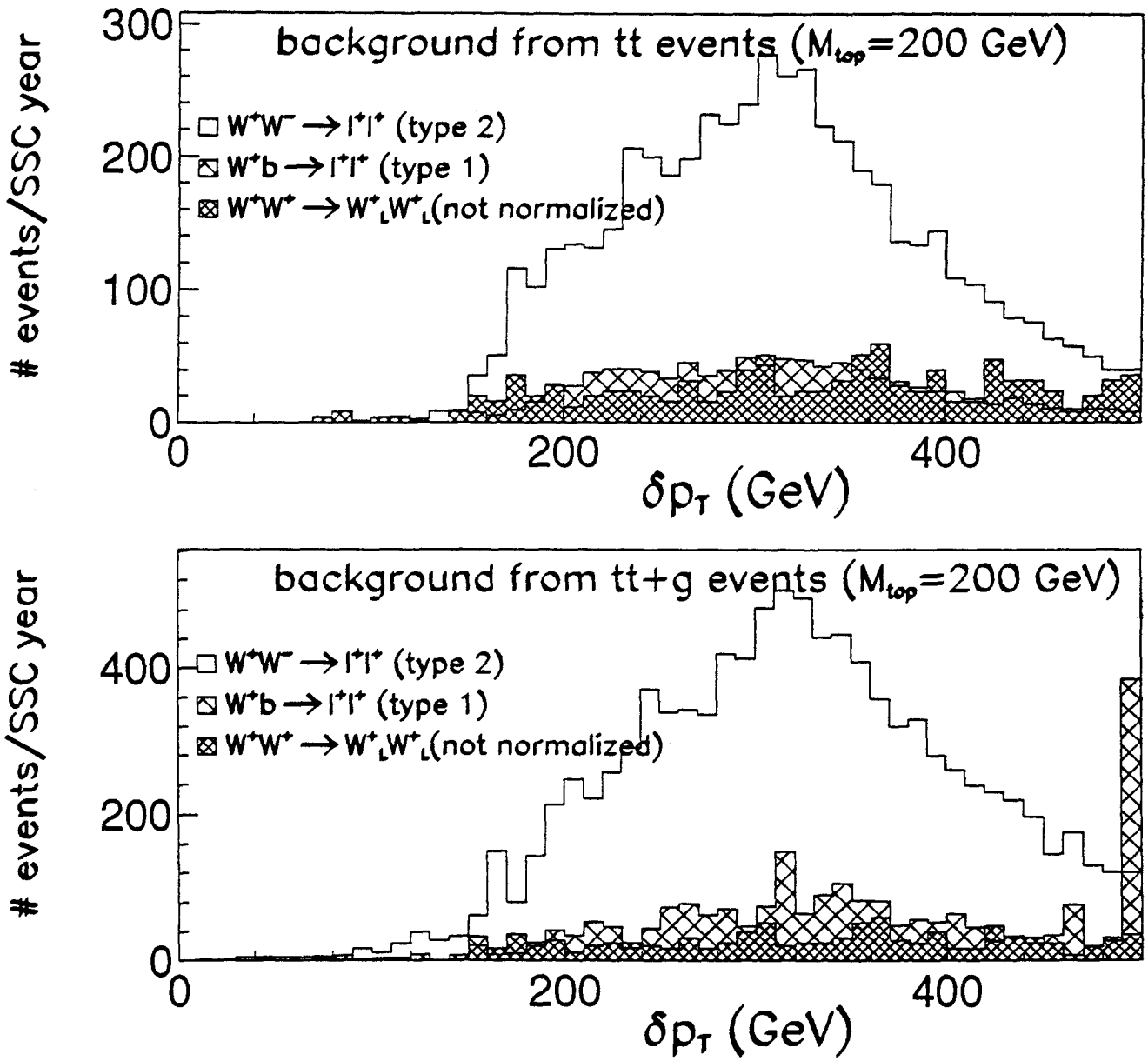

Figure 8: Vector difference of p_T between the two leptons in $t\bar{t}$ and $t\bar{t}+g$ background events, m_{top} = 200 GeV. The unnormalized signal is shown for comparison.

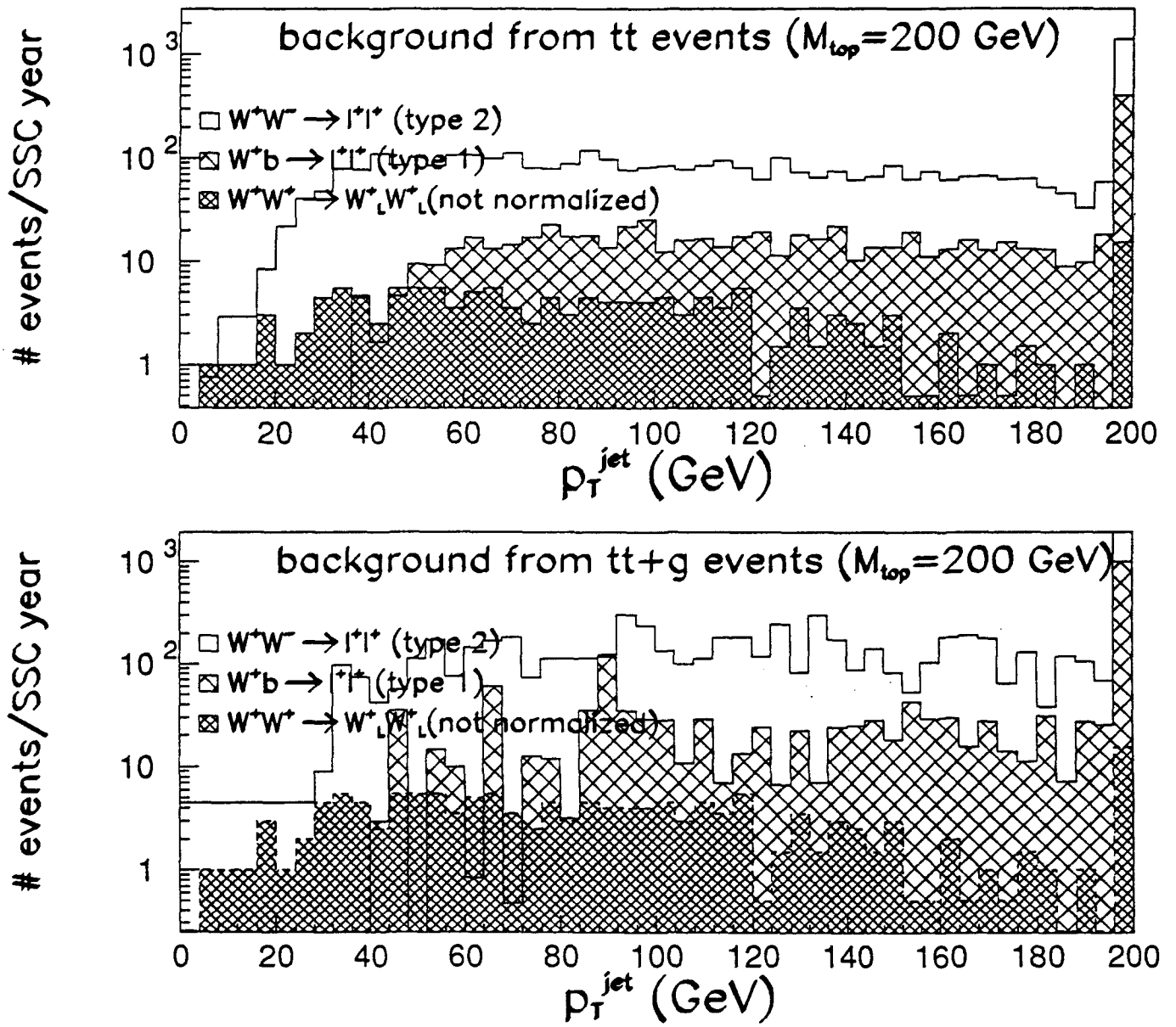

Figure 9: p_T of largest p_T jet in the event for $t\bar{t}$ background events, m_{top} = 200 GeV. The unnormalized signal is shown for comparison.

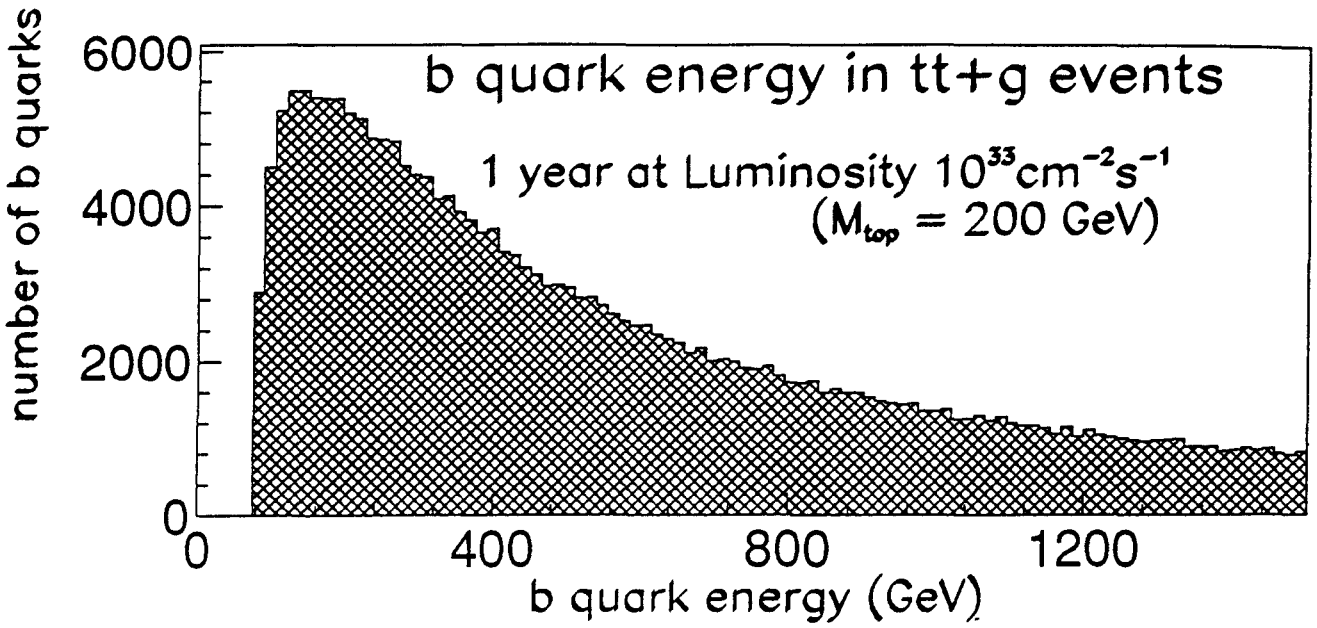

Figure 10: b quark energy for b quarks in $t\bar{t}$+g events.

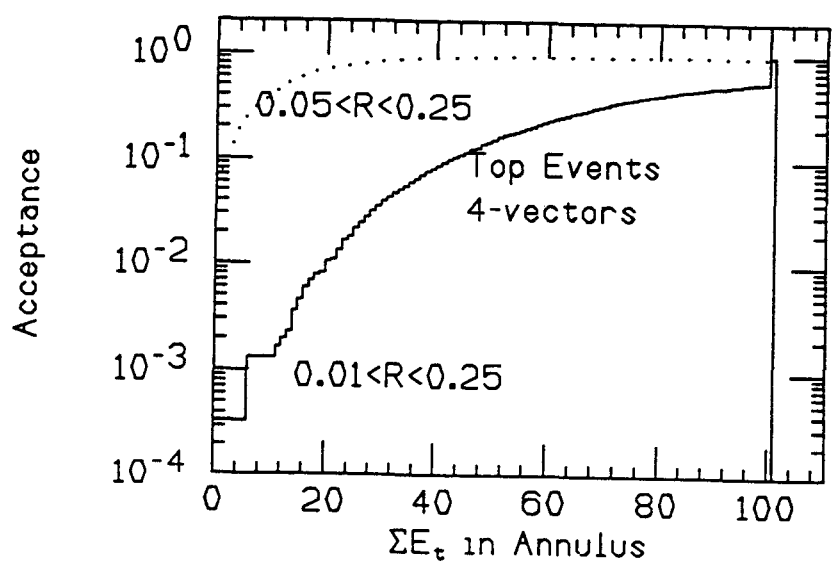

Figure 11: Fraction of leptons surviving (looking isolated) as a function of total energy cut for two different annuli(0.01< R <0.25 and 0.05 <R< 0.25) around the lepton in b jets using 4-vectors only.

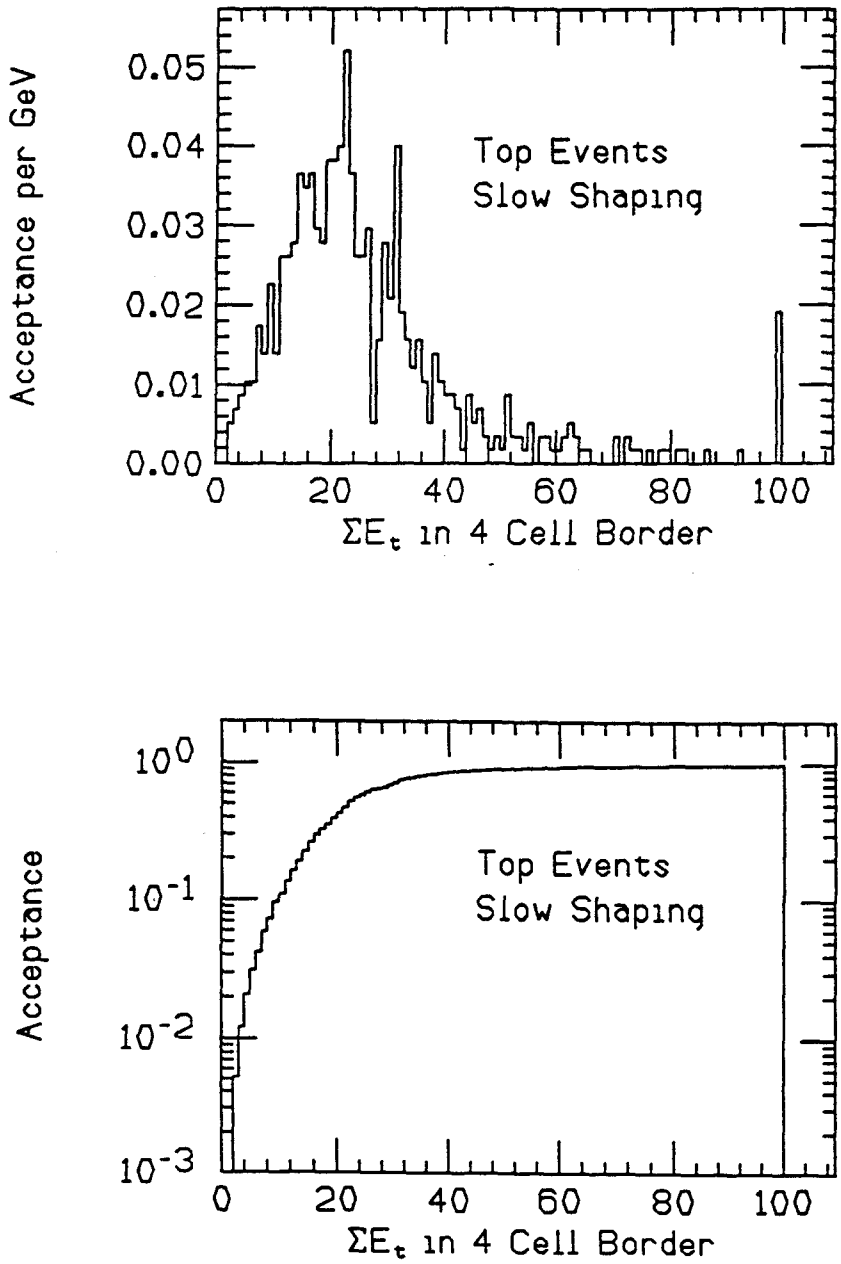

Figure 12: Fraction of leptons surviving (looking isolated) as a function of total energy cut for two different annuli($0.01 < R < 0.25$ and $0.05 < R < 0.25$) around the lepton in b jets using parametrized showers in the calorimeters for b jets in $t\bar{t}$ events.

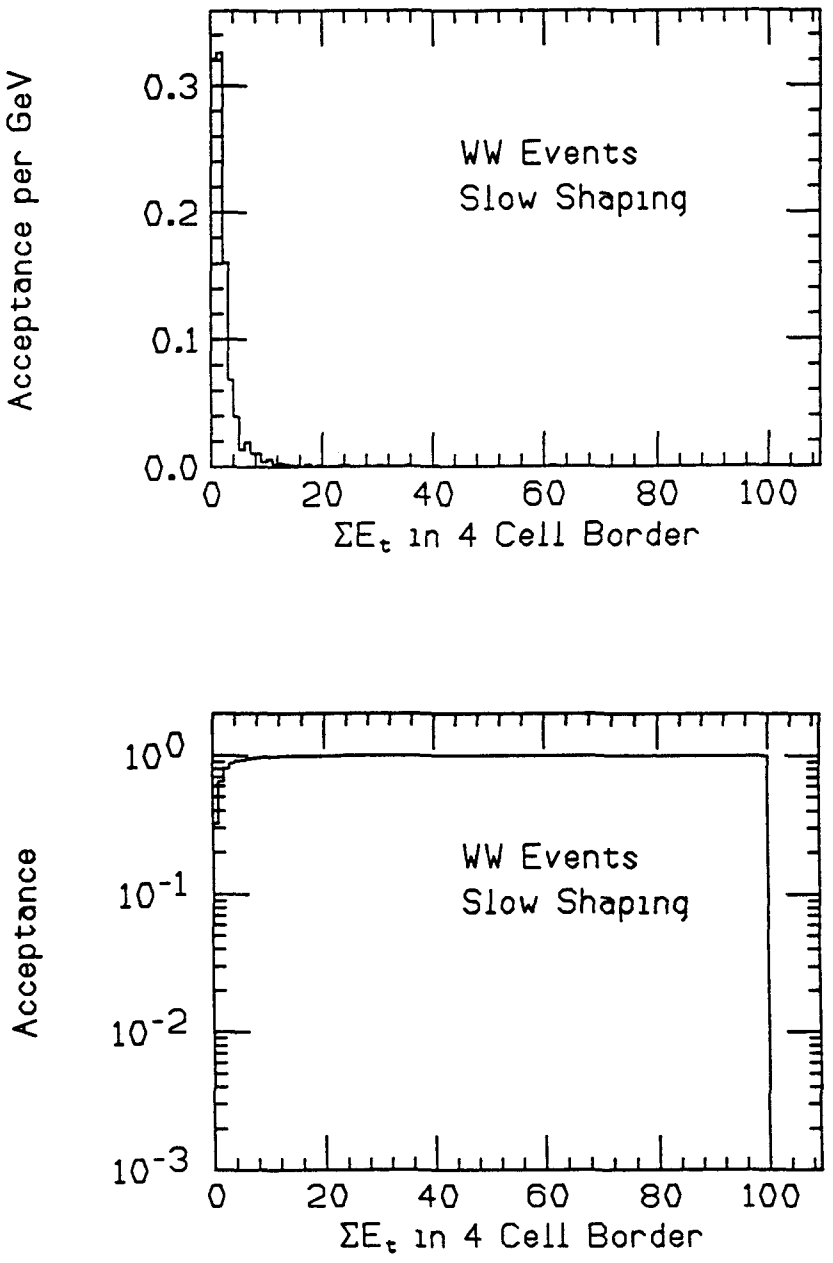

Figure 13: Fraction of leptons surviving (looking isolated) as a function of total energy cut for two different annuli($0.01 < R < 0.25$ and $0.05 < R < 0.25$) around the lepton using parametrized showers in the calorimeters for $W_L W_L$ signal events.

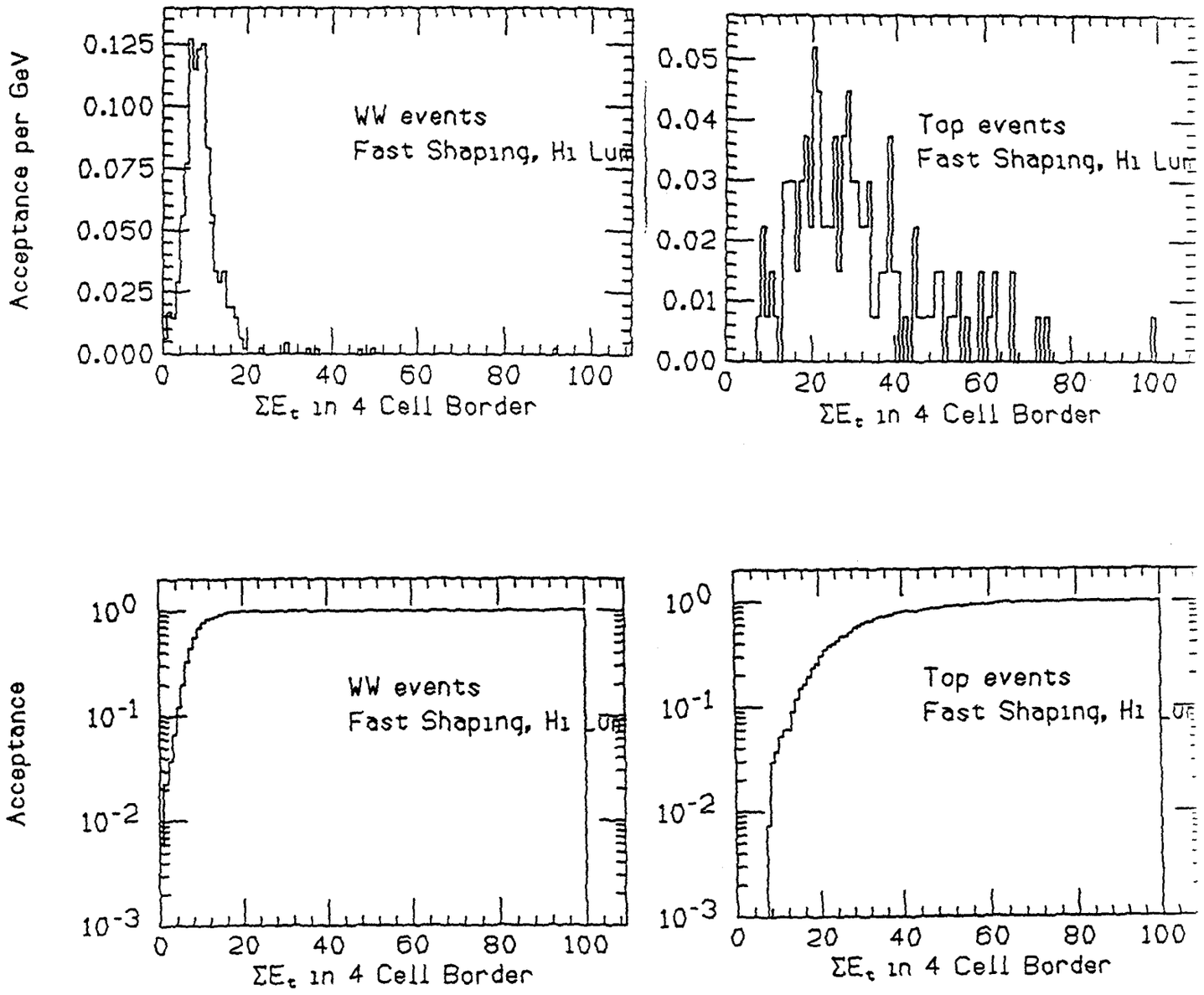

Figure 14: Isolation plots for WW signal and $t\bar{t}$ background for high luminosity running.

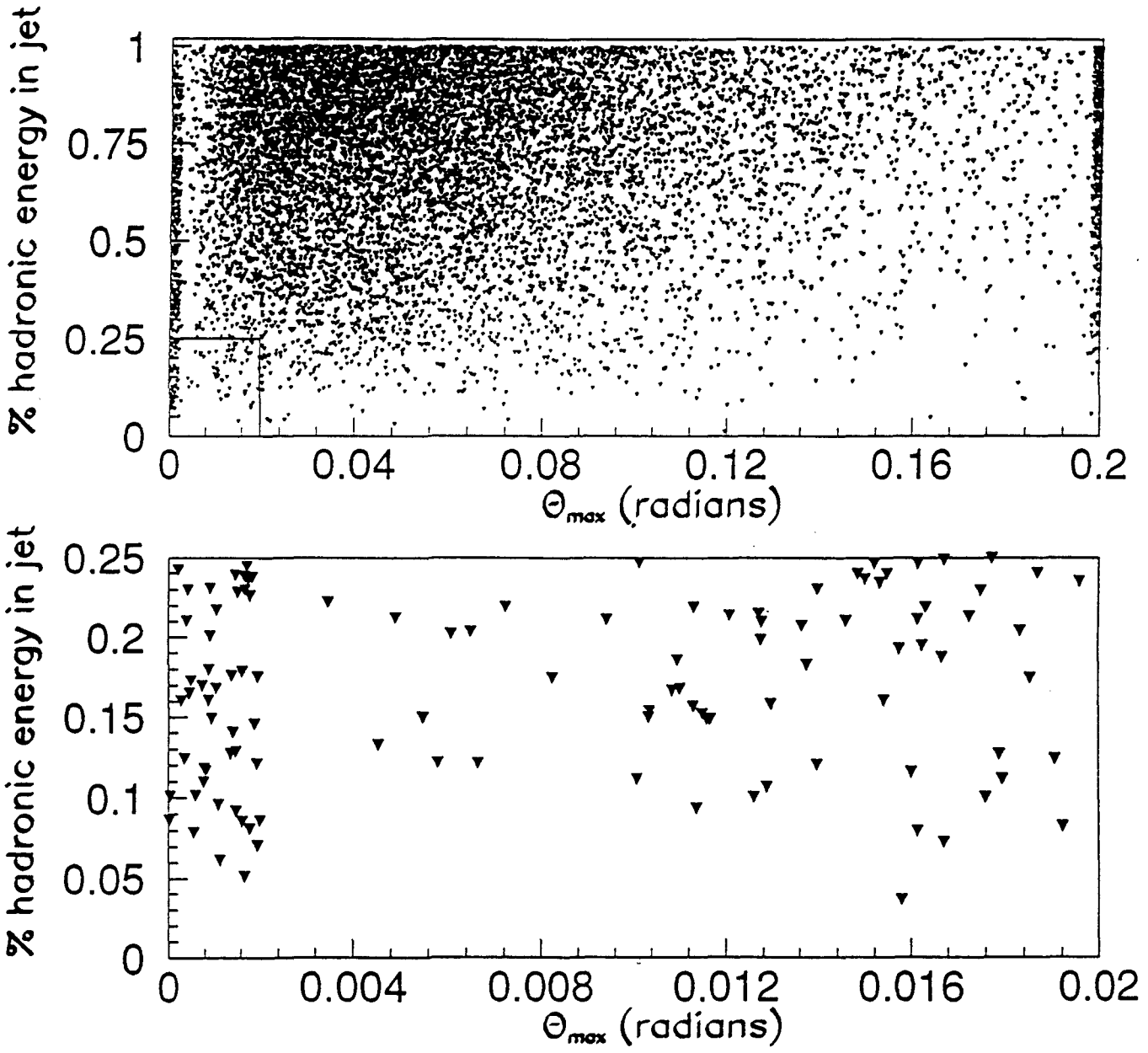

Figure 15: Angle between the two most separated charged tracks in a b jet vs. hadronic energy in the jet. The lower plot contains 1.0 % of the upper plots' entries.

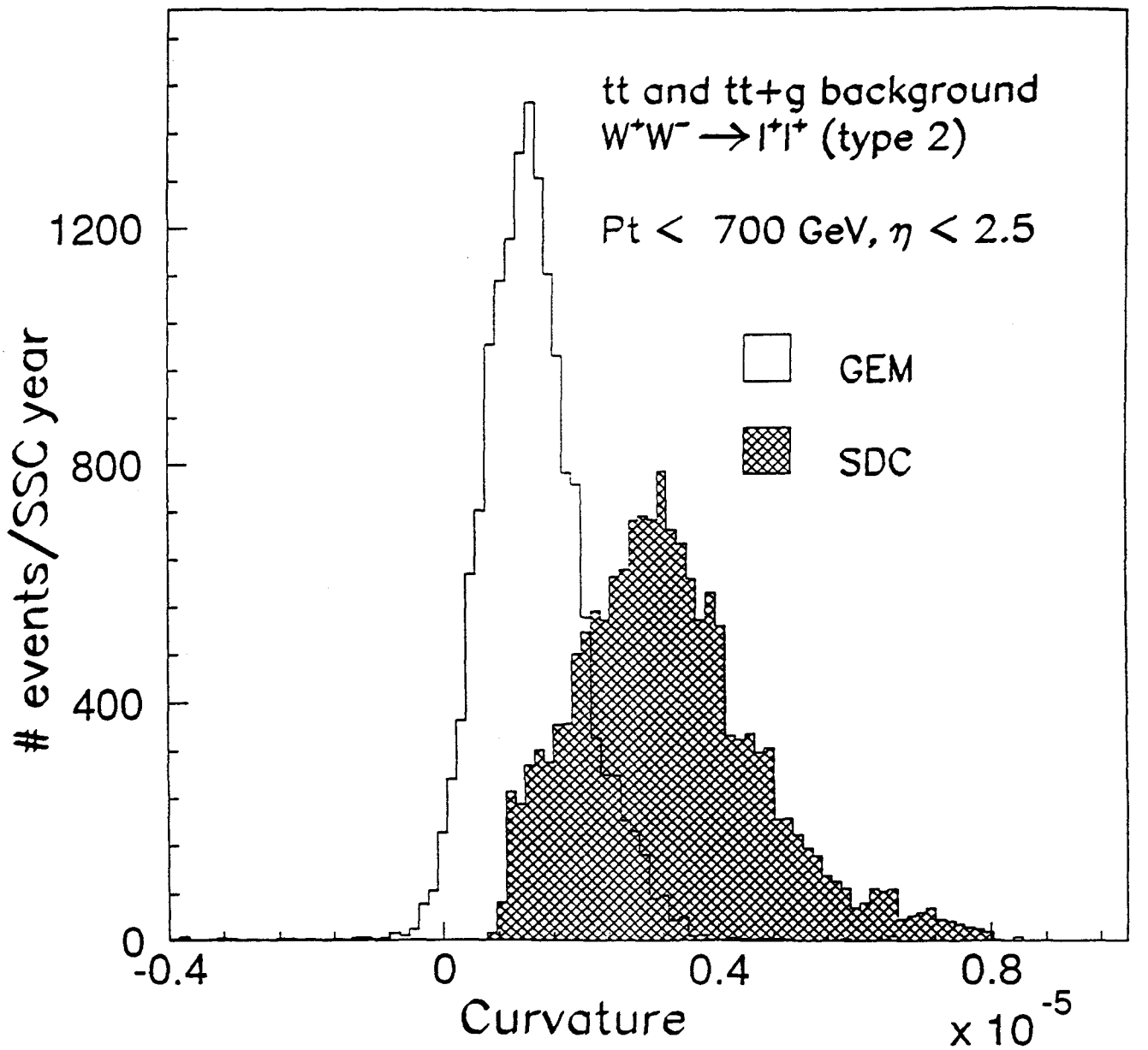

Figure 16: Curvature for type 2 $t\bar{t}$ background for the SDC and GEM geometries